$R^2 = R^3 = CH_3$), 99656-46-9; I (M = Co^{III}, $R^1 = (CH_3)_2$, $R^2 = R^3 = CH_3$), 99656-65-2; I (M = Co^{II}, $R^1 = (CH_2)_8$, $R^2 = R^3 = CH_3$), 97059-51-3; I (M = Co^{III}, $R^1 = (CH_2)_8$, $R^2 = R^3 = CH_3$), 99656-66-3; I (M = Co^{II}, $R^1 = (CH_2)_7$, $R^2 = R^3 = CH_3$), 97042-96-1; I (M = Co^{III}, $R^1 = (CH_2)_7$, $R^2 = R^3 = CH_3$), 99656-67-4; I (M = Co^{II}, $R^1 = (CH_2)_6$, $R^2 = R^3 = CH_3$), 73914-17-7; I (M = Co^{III}, $R^1 = (CH_2)_6$, $R^2 = R^3 = CH_3$), 99656-68-5; I (M = Co^{II}, $R^1 = (CH_2)_5$, $R^2 = R^3 = CH_3$), 99656-47-0; I (M = Co^{III}, $R^1 = (CH_2)_5$, $R^2 = R^3 = CH_3$), 73914-26-8; I (M = Co^{II}, $R^1 = (CH_2)_4$, $R^2 = R^3 = CH_3$), 99656-48-1; I (M = Co^{III}, $R^1 = (CH_2)_4$, $R^2 = R^3 = CH_3$), 73914-22-4; I (M = Co^{II}, $R^1 = (CH_2)_3$, $R^2 = R^3 = CH_3$), 97059-49-9; I (M = Co^{III}, $R^1 = (CH_2)_3$, $R^2 = R^3 = CH_3$), 99656-69-6; I (M = Fe^{II}, $R^1 = (CH_2)_3$, $R^2 = R^3 = CH_3$), 99656-92-5; I (M = Fe^{III}, $R^1 = (CH_2)_3$, $R^2 = R^3 = CH_3$), 99656-93-6; I (M = Fe^{II}, $R^1 = (CH_2)_4$, $R^2 = R^3 = CH_3$), 99656-94-7; I (M = Fe^{III}, $R^1 = (CH_2)_4$, $R^2 = R^3 = CH_3$), 99656-95-8; I (M = Fe^{II}, $R^1 = (CH_2)_5$, $R^2 = R^3 = CH_3$), 99656-96-9; I (M = Fe^{III}, $R^1 = (CH_2)_5$, $R^2 = R^3 = CH_3$), 99656-97-0; I (M = Fe^{II}, $R^1 = (CH_2)_6$, $R^2 = R^3 = CH_3$), 99656-98-1; I (M = Fe^{III}, $R^1 = (CH_2)_6$, $R^2 = R^3 = CH_3$), 99656-99-2; I (M = Ni^{II}, $R^1 = (CH_2)_4$, $R^2 = CH_3$, $R^3 = C_6H_5$), 88610-64-4; I (M = Ni^{III}, $R^1 = (CH_2)_4$, $R^2 = CH_3$, $R^3 = C_6H_5$), 99656-74-3; I (M = Ni^{II}, $R^1 = (CH_2)_5$, $R^2 = CH_3$, $R^3 = C_6H_5$), 88610-70-2; I (M = Ni^{III}, $R^1 = (CH_2)_5$, $R^2 = CH_3$, $R^3 = C_6H_5$), 99656-75-4; I (M = Ni^{II}, $R^1 = (CH_2)_6$, $R^2 = CH_3$, $R^3 = C_6H_5$), 88610-76-8; I (M = Ni^{III}, $R^1 = (CH_2)_6$, $R^2 = CH_3$, $R^3 = C_6H_5$), 99656-76-5; I (M = Ni^{II}, $R^1 = (CH_2)_7$, $R^2 = CH_3$, $R^3 = C_6H_5$), 88610-84-8; I (M = Ni^{III}, $R^1 = (CH_2)_7$, $R^2 = CH_3$, $R^3 = C_6H_5$), 99656-77-6; I (M = Co^{II}, $R^1 = (CH_2)_4$, $R^2 = CH_3$, $R^3 = C_6H_5$), 99656-78-7; I (M = Co^{III}, $R^1 = (CH_2)_4$, $R^2 = CH_3$, $R^3 = C_6H_5$), 99656-79-8; I (M = Co^{II}, $R^1 = (CH_2)_5$, $R^2 = CH_3$, $R^3 = C_6H_5$), 99656-80-1; I (M = Co^{III}, $R^1 = (CH_2)_5$, $R^2 = CH_3$, $R^3 = C_6H_5$), 99656-81-2; I (M = Co^{II}, $R^1 = (CH_2)_6$, $R^2 = CH_3$, $R^3 = C_6H_5$), 99656-82-3; I (M = Co^{III}, $R^1 = (CH_2)_6$, $R^2 = CH_3$, $R^3 = C_6H_5$), 99656-83-4; I (M = Co^{II}, $R^1 = (CH_2)_7$, $R^2 = CH_3$, $R^3 = C_6H_5$), 99656-84-5; I (M = Co^{III}, $R^1 = (CH_2)_7$, $R^2 = CH_3$, $R^3 = C_6H_5$), 99656-85-6; I (M = Fe^{II}, $R^1 = (CH_2)_4$, $R^2 = CH_3$, $R^3 = C_6H_5$), 99656-86-7; I (M = Fe^{III}, $R^1 = (CH_2)_4$, $R^2 = CH_3$, $R^3 = C_6H_5$), 99656-87-8; I (M = Fe^{II}, $R^1 = (CH_2)_5$, $R^2 = CH_3$, $R^3 = C_6H_5$), 99656-88-9; I (M = Fe^{III}, $R^1 = (CH_2)_5$, $R^2 = CH_3$, $R^3 = C_6H_5$), 99656-89-0; I (M = Fe^{II}, $R^1 = (CH_2)_6$, $R^2 = CH_3$, $R^3 = C_6H_5$), 99656-90-3; I (M = Fe^{III}, $R^1 = (CH_2)_6$, $R^2 = CH_3$, $R^3 = C_6H_5$), 99656-91-4; II (M = Ni^{II}, $R^1 = (CH_3)_2$, $R^2 = R^3 = CH_3$), 99685-53-7; II (M = Ni^{III}, $R^1 = (CH_3)_2$, $R^2 = R^3 = CH_3$), 99656-61-8; II (M = Ni^{II}, $R^1 = (CH_2)_{12}$, $R^2 = R^3 = CH_3$), 99656-44-7; II (M = Ni^{III}, $R^1 = (CH_2)_{12}$, $R^2 = R^3 = CH_3$), 99656-62-9; II (M = Ni^{II}, $R^1 = (CH_2)_8$, $R^2 = R^3 = CH_3$), 99656-45-8; II (M = Ni^{III}, $R^1 = (CH_2)_8$, $R^2 = R^3 = CH_3$), 99656-63-0; II (M = Ni^{II}, $R^1 = (CH_2)_6$, $R^2 = R^3 = CH_3$), 76791-42-9; II (M = Ni^{III}, $R^1 = (CH_2)_6$, $R^2 = R^3 = CH_3$), 99656-64-1; II (M = Co^{II}, $R^1 = (CH_3)_2$, $R^2 = R^3 = CH_3$), 99656-49-2; II (M = Co^{III}, $R^1 = (CH_3)_2$, $R^2 = R^3 = CH_3$), 99656-70-9; II (M = Co^{II}, $R^1 = (CH_2)_8$, $R^2 = R^3 = CH_3$), 99656-50-5; II (M = Co^{III}, $R^1 = (CH_2)_8$, $R^2 = R^3 = CH_3$), 99656-71-0; II (M = Co^{II}, $R^1 = (CH_2)_7$, $R^2 = R^3 = CH_3$), 99656-51-6; II (M = Co^{III}, $R^1 = (CH_2)_7$, $R^2 = R^3 = CH_3$), 99656-72-1; II (M = Co^{II}, $R^1 = (CH_2)_6$, $R^2 = R^3 = CH_3$), 99656-52-7; II (M = Co^{III}, $R^1 = (CH_2)_6$, $R^2 = R^3 = CH_3$), 99656-73-2; (TBA)BF_4, 429-42-5; O_2, 7782-44-7.

Contribution from the Dipartimento di Chimica Generale, Università di Pavia, 27100 Pavia, Italy, and Institut für Anorganische Chemie, Universität Basel, 4056 Basel, Switzerland

Complexation of Divalent and Trivalent Nickel and Copper Ions by Rigid and Flexible Dioxo Tetraaza Macrocycles

Luigi Fabbrizzi,*[1a] Thomas A. Kaden,*[1b] Angelo Perotti,[1a] Barbara Seghi,[1a] and Liselotte Siegfried[1b]

Received July 2, 1985

Potentiometric, spectrophotometric, kinetic, and electrochemical studies on the Ni^{2+} and Cu^{2+} complexes with the two macrocycles **1** and **2** have been performed to investigate the importance of the flexibility of the macrocyclic ring to the properties of the corresponding complexes. The more flexible ligand **1** gives a series of Cu^{2+} complexes with variable protonation stoichiometry, whereas ligand **2** only forms a Cu^{2+} complex of the type [$CuLH_{-2}$]. The two ligands also differ in their complexation kinetics, the reactivity of **1** being higher than that of **2**. Thus from its equilibria and kinetics, ligand **1** closely resembles open-chain ligands, whereas the reactivity of **2** is typical for macrocycles. On the other hand, the redox potential of the M(III)/M(II) couple is practically independent of the rigidity of the macrocyclic ring.

Introduction

The study of metal complexes with tetraaza macrocycles has been developed from the thermodynamic[2] as well as from the kinetic point of view.[3] With the report of the synthesis of dioxo tetraaza macrocycles by Tabushi et al.[4] and the complexation studies of these ligands with Ni^{2+} and Cu^{2+} by Kimura et al.,[5,6] new and interesting properties of these macrocycles have been observed. So dioxo tetraaza macrocycles (a) can coordinate Ni^{2+} and Cu^{2+} with dissociation of two protons from the amido groups,[5,6] giving neutral complexes MLH_{-2}, (b) exhibit dissociation kinetics that are relatively fast compared to those of the analogous tetraamine macrocyclic compelxes,[7] and (c) form Ni^{2+} and Cu^{2+} complexes that can be electrochemically oxidized to give trivalent species, sometimes stable even in aqueous solution.[6,8,9]

Most of the dioxo macrocycles studied up to now have two amide groups cis to each other (ligands **3** and **4**). These ligands have the advantage of a relatively rigid structure when the two amide groups are deprotonated and thus produce strong ligand fields.

However, there are in the literature also a few dioxo macrocycles with trans amide groups, such as ligands **1** and **2**, and their complexation properties have only partially been studied.

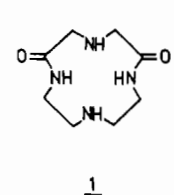

1

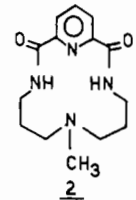

2

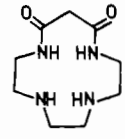

3

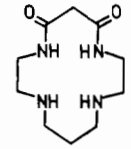

4

We report here a series of equilibrium measurements, the kinetics of formation and dissociation of their Ni^{2+} and Cu^{2+}

(1) (a) Università di Pavia. (b) Universität Basel.
(2) Fabbrizzi, L.; Micheloni, M.; Paoletti, P. *Inorg. Chem.* **1980**, *19*, 535–538.
(3) Leugger, A.; Hertli, L.; Kaden, Th. A. *Helv. Chim. Acta* **1978**, *61*, 2296–2306.
(4) Tabushi, I.; Taniguchi, Y.; Kato, H. *Tetrahedron Lett.* **1977**, *18*, 1049–1052.
(5) Kodama, M.; Kimura, E. *J. Chem. Soc., Dalton Trans.* **1979**, 325–329.
(6) Kodama, M.; Kimura, E. *J. Chem. Soc., Dalton Trans.* **1981**, 694–700.
(7) Hay, R. W.; Pujari, M. P.; McLaren, F. *Inorg. Chem.* **1984**, *23*, 3033–3035.
(8) Fabbrizzi, L.; Poggi, A. *J. Chem. Soc., Chem. Commun.* **1980**, 646–647.
(9) Fabbrizzi, L.; Perotti, A.; Poggi, A. *Inorg. Chem.* **1983**, *22*, 1411–1412.

0020-1669/86/1325-0321$01.50/0

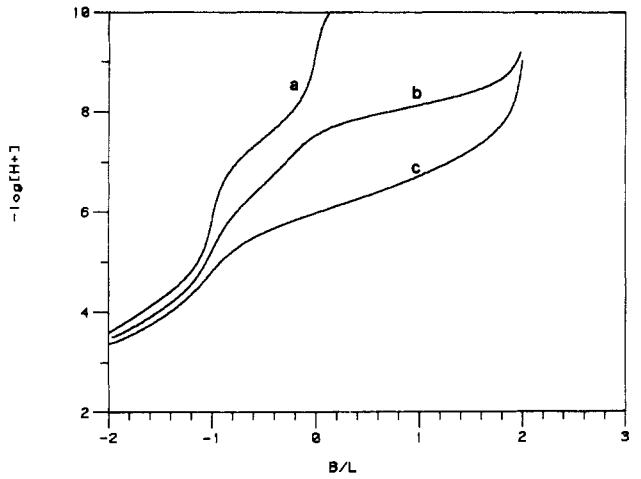

Figure 1. Titration curves: (a) ligand **1** + 2 equiv of acid; (b) **1** + 2 equiv of acid + 1 equiv of Ni^{2+}; (c) **1** + 2 equiv of acid + 1 equiv of Cu^{2+}. B/L is the ratio of moles of standard base added, B, over the moles of ligand **1**. Negative values indicate excess of acid (e.g., −1 = 1 equiv of standard acid).

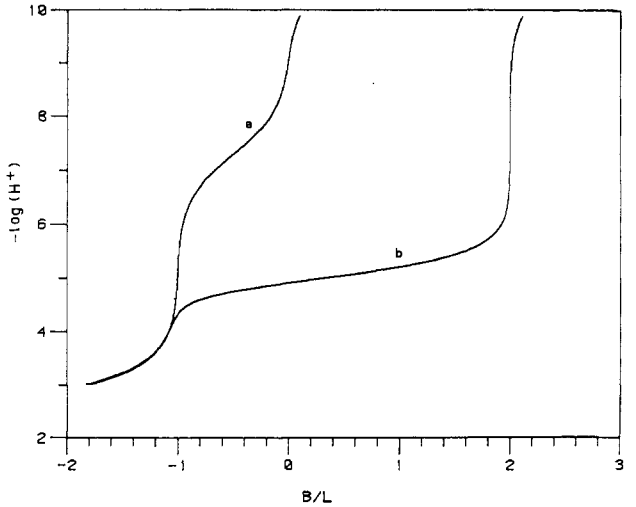

Figure 2. Titration curves: (a) ligand **2** + 2 equiv of acid; (b) **2** + 2 equiv of acid + 1 equiv of Cu^{2+}. B/L is as in Figure 1.

complexes, and their electrochemistry in order to point out similarities and differences between the two ligands **1** and **2**, as well as those between dioxo macrocycles with trans (**1** and **2**) and cis (**3** and **4**) arrangements of the amide groups.

The solution chemistry of the Ni^{2+} and Cu^{2+} complexes of the 12-membered macrocycle **1** was previously reported by Kimura et al.[6] This investigation enables us to demonstrate through careful computer analysis of potentiometric and spectrophotometric titration data the existence of additional species present in the metal–ligand equilibria and thus supplements earlier results.

Experimental Section

Syntheses of the Dioxo Tetraaza Macrocycles. **1** was prepared by condensation of the dimethyl ester of iminodiacetic acid and diethylenetriamine in ethanol (5×10^{-2} M scale; refluxed for 5 days). The solution, concentrated to $^1/_{20}$th of its original volume, gave on standing a precipitate, which was crystallized from ethanol (yield 10%); mp 164–166 °C (lit. mp 163–165 °C).[6] **2** was obtained by following the procedure described by Vögtle et al.; mp 165–166 °C (lit. mp 164–166 °C).[10]

Potentiometric Measurements. The potentiometric titrations of the ligands in the presence and in the absence of metal ions (as perchlorate salts) were carried out in an automatic system controlled by an Apple IIe computer and consisting of (i) a Radiometer PMH84 research pH meter, using a Beckman Futura glass electrode and an Ingold saturated sodium chloride–calomel reference electrode fitted in an Ingold cell system, (ii) a Radiometer ABU80 Autoburette, (iii) a Metrohm thermostated cell, and (iv) a Huber MINISTAT digital thermostat.

The temperature was maintained at 25.0 ± 0.1 °C. Each titration was performed on a 50-cm^3 solution adjusted to 0.1 M ionic strength with $NaClO_4$ (a few measurements were also done in 0.5 M KNO_3).

In this way the concentrations of the hydrogen ions were monitored.[11a]

Typical concentrations of the ligands and metal ions (in a 1:1 molar ratio) were in the range of $(0.5–1.0) \times 10^{-3}$ M. The details of the experimental procedure have been extensively described elsewhere.[12] The data were processed on a VAX 11/780 computer using the MINIQUAD program[13] and the constants expressed in terms of concentration quotients.[11b]

Typical titration curves are shown in Figures 1 and 2.

Spectrophotometric Titrations. The spectrophotometric titrations of the Cu^{2+} complex with **1** were run on the fully automatic spectrophotometric titration apparatus described previously.[14] The starting solution was a mixture of 5×10^{-3} M **1** and 4.5×10^{-3} M Cu^{2+} acidified to pH 2 and kept with KNO_3 to $I = 0.5$. The pH was changed by stepwise addition of 0.2 M NaOH to 2 mL of starting solution in the cell. After each addition, the spectra were recorded from 800 to 460 nm, and the pH was measured. The calculations of the equilibrium constants and the distribution of the species were performed with the computer program SPECFIT.[15]

Kinetic Measurements. The rates of complex formation and dissociation with **1** were measured with a Durrum D110 stopped-flow instrument equipped with a Datalab DL901 transient recorder on line with a Rockwell computer. Rate constants were calculated on line as pseudo-first-order rates. To cover the pH region several buffers were used (all 0.05 M): 5.9–7.8, 2,6-lutidine; 7.0–9.5, *N*-methylmorpholine; 9.5–10.5, (*tert*-butylamino)ethanol.

Typical concentrations were $[Ni^{2+}] = 4.5 \times 10^{-4}$ M, $[\mathbf{1}] = 5 \times 10^{-4}$ M, and $[KNO_3] = 0.5$ M, either at a starting pH of 11 for dissociation measurements or at pH 5 for formation measurements. The reactions were followed at 460 nm.

The kinetics with **1** were measured on a Varian Techtron spectrophotometer at 518 nm. Typical concentration conditions for the dissociation were 8×10^{-4} M Cu^{2+} complex that was mixed with HNO_3 of different concentrations to cover the pH range 0.3–1.8. With KNO_3 the ionic strength was kept constant at 0.5 M.

For complex formation, 5×10^{-4} M **2** and 5×10^{-3} M Cu^{2+} were reacted in 0.05 2,6-lutidine-3-sulfonic acid buffer. This buffer did not affect the reaction rate, since it forms no complexes with Cu^{2+} under these conditions.[16] Rate constants were calculated as pseudo first order (since $[Cu^{2+}] = 10 \times [\mathbf{2}]$) and converted to second-order constants taking into account the $[Cu^{2+}]$ used.

Electrochemistry. Cyclic voltammetry experiments were performed with a three-electrode assembly as previously described.[17] The working electrode was a carbon-paste electrode, which gave reversible profiles for both nickel and copper complexes. In the case of the copper complexes, the platinum microsphere working electrode gave reversible responses whereas, in the case of nickel, ill-defined, poorly reversible profiles were obtained.

Solutions for electrochemistry were prepared immediately before experiments, from stoichiometric amounts of the ligand and standard solutions of the metal salts; standard NaOH was added to adjust the solution to the minimum pH at which the $[MLH_{-2}]$[18] species was present at 100%. The ionic strength was adjusted to 0.1 M with $NaClO_4$. The cell was thermostated at 25 ± 0.1 °C.

The spectra of the Cu^{III} complexes generated through controlled-potential electrolysis (using platinum gauze as an anode) were recorded on

(10) Vögtle, F.; Zeber, E.; Wehner, W.; Naetscher, R.; Gruetze, J. *Chem.-Ztg.* **1974**, *98*, 562.
(11) (a) Rossotti, H. "The Study of Ionic Equilibria"; Longman: London, 1978; p 19. (b) *Ibid.*, p 17.
(12) Fabbrizzi, L.; Forlini, F.; Perotti, A.; Seghi, B. *Inorg. Chem.* **1984**, *23*, 807–813.
(13) Sabatini, A.; Vacca, A.; Gans, P. *Talanta* **1974**, *21*, 53–77.
(14) Hänisch, G.; Zuberbühler, A. D.; Kaden, Th. A. *Talanta* **1979**, *26*, 563–567.
(15) Gampp, H.; Maeder, M.; Mayer, C. J.; Zuberbühler, A. D. *Talanta* **1985**, *32*, 257.
(16) Bips, U.; Elias, H.; Hauroder, M.; Kleinhans, G.; Pfeifer, S.; Wannowius, K. J. *Inorg. Chem.* **1983**, *22*, 3862–3865.
(17) Buttafava, A.; Fabbrizzi, L.; Perotti, A.; Poggi, A.; Seghi, B. *Inorg. Chem.* **1984**, *23*, 3917–3922.
(18) In the text every dioxo tetraaza ligand is denoted as L; an LH_p formula denotes protonated ($p > 0$) or deprotonated ($p < 0$) species; for instance, the $[MLH_{-2}]$ formula indicates the metal complex in which the M^{2+} ion is coordinated by the twice deprotonated ligand.

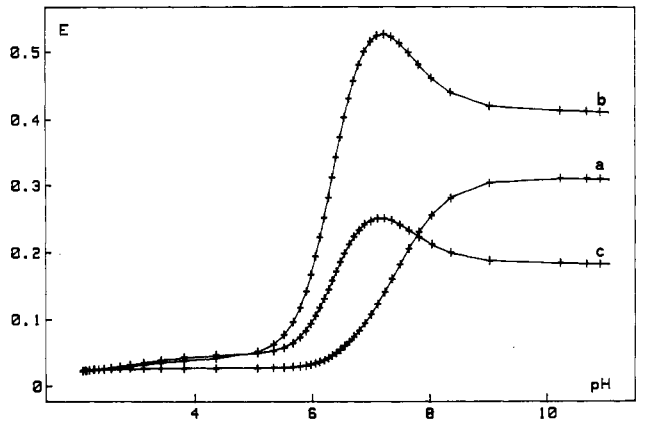

Figure 3. Spectrophotometric titration of 5.2×10^{-3} M **1** and 4.7×10^{-3} M Cu^{2+} at 480 nm (a), 660 nm (b), and 800 nm (c). Both the experimental points and the theoretical curve calculated with the constants of Table I (for 0.5 M KNO_3) are shown.

a Cary 2300 spectrophotometer using a 1-mm quartz cell.

Results and Discussion

Protonation Equilibria. The protonation equilibria of both ligands (**1** and **2**) are shown in eq 1 and 2, and the corresponding

$$H^+ + L \rightleftharpoons LH^+ \quad (1)$$

$$H^+ + LH^+ \rightleftharpoons LH_2^{2+} \quad (2)$$

log K values are reported in Table I, in which the values for the previously investigated *trans*-dioxo tetraaza macrocycles **3** and **4** are also given.

The log K_1 values of the dioxo ligands decrease along the series **4**, **3**, **1**, which is the order of decreasing ring size. Since log K_1 values of **4**, **3**, and **1** all describe the basicity of a secondary amino group, such a trend would not be expected and could indicate differences in solvation. The 14-membered ligand **2** containing the pyridine ring presents the smallest log K_1: it should be noted that protonation here involves a tertiary rather than a secondary amine nitrogen atom and that the rigid nature of the molecule could lower the basicity.

Whereas for **2** the second protonation constant log K_2 is below 1.50, due to the presence of the less basic pyridine nitrogen atom, the value for **1** can be measured and it is worthwhile to compare the behavior of **1** with that of the other dioxo macrocycles **3** and **4**. For **4** and **3**, large values of $\Delta \log K_{12} = \log K_1 - \log K_2$ are observed (3.71 and 4.66 for **4** and **3**, respectively), which have been already interpreted[17] in terms of an electrostatic repulsive effect between the two protonated amino nitrogen atoms in cis positions. For **1**, $\Delta \log K_{12}$ is only 3.31 log units, i.e., 0.40 and 1.35 log unit less than for **4** and **3**, respectively, although the ring is smaller. This can be understood considering that in this molecule the two protonated amino nitrogen atoms are trans to each other and thus the electrostatic repulsion is lower.

It should be also noted that the first protonation steps in **1** and **2** are much weaker than those of their fully saturated analogous 1,4,7,10-tetraazacyclododecane (log K_1 = 10.97)[3] and 2,7,12-trimethyl-3,7,11,17-tetraazabicyclo[11.3.1]heptadeca-1-(17),13,15-triene (log K_1 = 10.21).[19]

Complexation of 1. (a) With the Copper (II) Ion. The coordinating tendency of **1** toward Cu(II) has been studied by means of potentiometric titrations (in 0.1 M $NaClO_4$ and 0.5 M KNO_3 solutions) and spectrophotometric measurements (in 0.5 M KNO_3 solutions). In both techniques the best fittings of the experimental results were obtianed with four complexes, namely $[CuLH]^{3+}$, $[CuL]^{2+}$, $[CuLH_{-1}]^+$, and $[CuLH_{-2}]$, whose formation constants are reported in Table I. The potentiometric titration curve is shown in Figure 1. Examples of the spectrophotometric titration

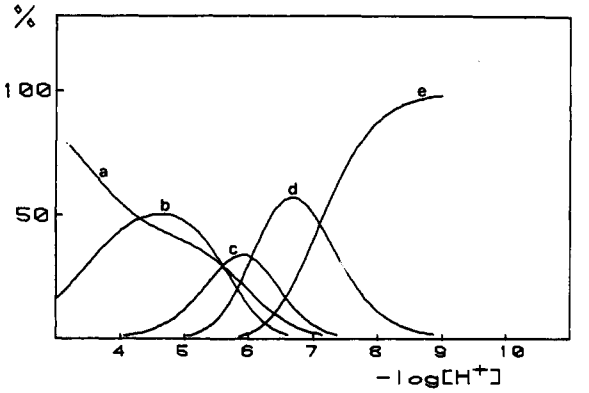

Figure 4. Distribution diagram for the system Cu^{2+}–**1** in equimolar amounts calculated with the constants of Table I (for 0.1 M $NaClO_4$): Cu^{2+} (a); $[CuLH]^{3+}$ (b); $[CuL]^{2+}$ (c); $[CuLH_{-1}]^+$ (d); $[CuLH_{-2}]$ (e).

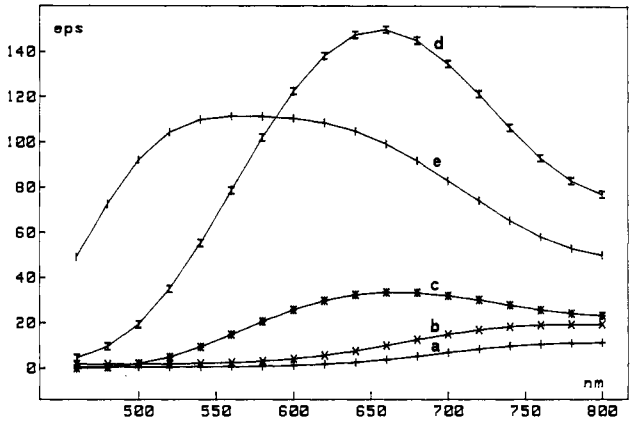

Figure 5. Absorption spectra of the species Cu^{2+} (a), $[CuLH]^{3+}$ (b), $[CuL]^{2+}$ (c), $[CuLH_{-1}]^+$ (d), and $[CuLH_{-2}]$ (e) for L = **1** calculated from the spectrophotometric titration with the program SPECFIT.

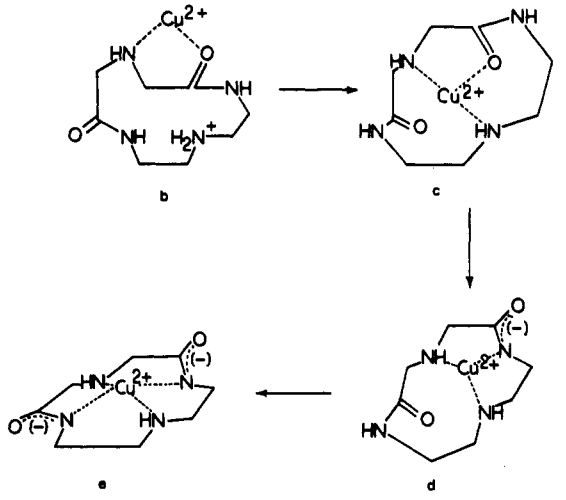

Figure 6. Proposed structures for the Cu^{2+} complexes with **1**: $[CuLH]^{3+}$ (b), $[CuL]^{2+}$ (c), $[CuLH_{-1}]^+$ (d) and $[CuLH_{-2}]$ (e).

at three selected wavelengths are given in Figure 3. The distribution curves of the species present at equilibrium are shown in Figure 4. Figure 5 exhibits the absorption spectra of the above complex species calculated by using the SPECFIT computer program.

$[CuLH]^{3+}$. This species, which reaches its maximum concentration (50%) at pH 4.5, absorbs at 786 nm (ϵ = 18). In this tripositive complex the proton is bound to one amino nitrogen, whereas the Cu(II) ion is coordinated by the other and, possibly, by the carbonyl oxygen of the adjacent amido group, as sketched in Figure 6.

$[CuL]^{2+}$. This species reaches a maximum concentration (40%) at pH 6. The shift of the absorption band toward lower wave

(19) Schultz-Grunow, P.; Kaden, Th. A. *Helv. Chim. Acta* **1978**, *61*, 2291–2296.

Table I. Equilibrium Constants (log Values) for the Stepwise Protonation and Complex Formation of Dioxo Tetraaza Macrocycles in Aqueous 0.1 M $NaClO_4$ and 0.5 M KNO_3, at 25 °C

equilibrium	1	2	3	4
$L + H^+ \rightleftharpoons LH^+$	7.48 ± 0.01 7.68 ± 0.01[d]	7.30 ± 0.01	8.78[a]	9.51[b]
$LH^+ + H^+ \rightleftharpoons LH_2^{2+}$	4.17 ± 0.01 4.40 ± 0.01[d]	<1.50	4.12[a]	5.80[b]
$Cu^{2+} + LH^+ \rightleftharpoons [CuLH]^{3+}$	3.45 ± 0.01 3.83 ± 0.01[d] 3.86 ± 0.02[d,e]			
$Cu^{2+} + L \rightleftharpoons [CuL]^{2+}$	5.34 ± 0.01 5.51 ± 0.01[d] 5.44 ± 0.02[d,e]		7.73[a]	8.75[b]
$Cu^{2+} + L \rightleftharpoons [CuLH_{-1}]^+ + H^+$	−0.69 ± 0.01 −0.78 ± 0.01[d] −0.86 ± 0.02[d,e]			
$Cu^{2+} + L \rightleftharpoons [CuLH_{-2}] + 2H^+$	−7.79 ± 0.01 −8.11 ± 0.01[d] −8.34 ± 0.01[d,e]	−4.64 ± 0.03	−2.02[a]	0.44[b]
$Ni^{2+} + LH^+ \rightleftharpoons [NiLH]^{3+}$	2.98 ± 0.01 3.49 ± 0.01[d]			
$Ni^{2+} + L \rightleftharpoons [NiL]^{2+}$	4.38 ± 0.01 4.66 ± 0.01[d]			
$Ni^{2+} + L \rightleftharpoons [NiLH_{-2}] + 2H^+$	−11.73 ± 0.03 −12.09 ± 0.03[d]		−6.40[c]	−6.00[c]

[a] Reference 16. [b] Reference 11. [c] Reference 22. [d] In 0.5 M KNO_3. [e] Spectrophotometric titration.

lengths (λ = 674 nm, ϵ = 26) would suggest[20] that both amine nitrogen atoms are bound to the copper ion.

$[CuLH_{-1}]^+$. The formation of this compelx, which reaches its maximum concentration (60%) at pH 7, involves the deprotontion of one of the two amido groups. This causes a remarkable increase in the molar absorptivity (λ_{max} = 659 nm, ϵ = 152).

$[CuLH_{-2}]$. In this species, which is completely formed at pH >8.5, all four nitrogen atoms (two amine groups and two deprotonated amido groups) are fully coordinated. The value of λ_{max} = 568 nm (ϵ = 108) is larger than those observed with $[CuLH_{-2}]$ complexes of the previously investigated dioxo tetraamines (**3**, 520 nm; **4**, 505 nm).[21] This weaker metal–ligand interaction can be ascribed to the fact that the 12-membered macrocyclic ring is too small to encompass the Cu^{2+} ion, which probably lies over the N_4 plane.

The region at higher pH has been investigated by spectrophotometric titrations in order to find evidence for possible hydrolytic tendencies of the complex. In contrast to the Kimura's report,[6] we do not observe formation of the hydrolyzed species $[CuLH_{-3}]^-$ up to pH 11 (see Figure 3). Above pH 11, however, there is an indication that a new species begins to form.

(b) With the Nickel(II) Ion. Figure 1 shows the titration curve obtained for the Ni^{II}–**1** system (1:1 molar ratio). The following species have been identified by computer analysis: $[NiLH]^{3+}$, $[NiL]^{2+}$, $[NiLH_{-2}]$.

Spectrophotometric titrations have shown that the species $[NiLH]^{3+}$ and $[NiL]^{2+}$ have low molar absorptivities (ϵ < 10), as expected for high-spin octahedral complexes. On the other hand, $[NiLH_{-2}]$ presents a band at 459 nm (ϵ = 83), typical of a diamagnetic square-planar chromophore. In contrast to the copper system the species $[NiLH_{-1}]^+$ does not form. This behavior, which has been previously observed for cyclic[22] and noncyclic[23] tetraaza ligands containing two amido groups, can be ascribed to the energy gain associated with the high-spin/low-spin transition when the two amido groups deprotonate. The proposed structures of the nickel species are analogous to those described for copper (Figure 6). The energy associated with the absorption band of the yellow $[NiLH_{-2}]$ species is remarkably lower than that observed for the corresponding complex with the 13-membered dioxo macrocycle **3** (413 nm),[22] indicating less strong metal–ligand interactions. This can be explained considering that the 13-membered cavity is tailor-made for low-spin Ni(II) whereas the 12-membered ring is too small and the 14-membered ring is too large to encompass this metal ion.

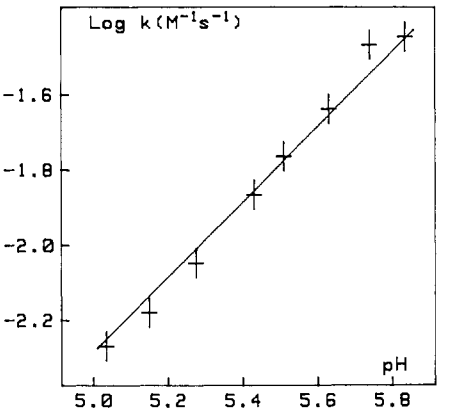

Figure 7. pH profile for the observed rate constant of the formation of $[CuLH_{-2}]$ with L = **2**.

Complexation of 2. The complexation of Cu^{2+} by **2** has been studied by pH titrations (Figure 2). The fitting of the experimental results is obtained by assuming the presence of only one species: $[CuLH_{-2}]$. Furthermore, in contrast to the measurements with **1**, complexation was found to be much slower, each titration point requiring up to 60 min to reach equilibrium.

The formation of only the neutral species $[CuLH_{-2}]$ as well as the sluggish metal incorporation can be explained by the relatively rigid nature of the ligand framework containing a pyridine ring and two adjacent amido groups (to give a set of three consecutive nitrogen atoms perfectly coplanar). The formation constant of the $[CuLH_{-2}]$ complex (−4.64 log units) is remarkably lower than that for the corresponding complex with the 14-membered ligand **4** (0.44 log unit), which instead of a pyridine nitrogen atom presents an amino group in the donor set and has a more favorable sequence of the chelate rings (5,6,5,6). The $[CuLH_{-2}]$ complex absorbs at 515 nm.

The titration curve for the Ni^{II}–**2** system superimposes with the titration curve of the free ligand up to the pH where $Ni(OH)_2$ precipitation occurs, indicating no complex formation at least in the time scale of the titration experiment.

(20) Billo, E. J. *Inorg. Nucl. Chem. Lett.* **1974**, *10*, 613–617.
(21) Kimura, E.; Koike, T.; Machida, R.; Nagai, R.; Kodama, M. *Inorg. Chem.* **1984**, *23*, 4181–4188.
(22) Fabbrizzi, L.; Perotti, A.; Poggi, A.; Seghi, B., to be submitted for publication.
(23) Kaden, Th. A.; Zuberbühler, A. D. *Helv. Chim. Acta* **1974**, *57*, 286–293.

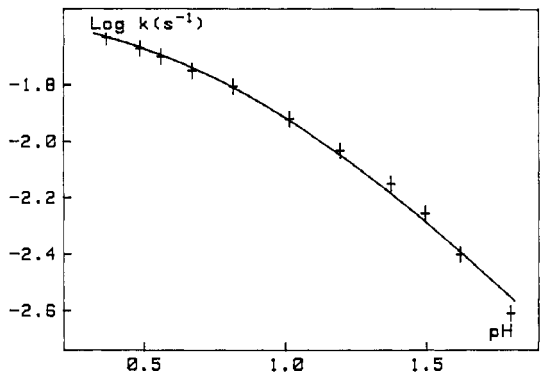

Figure 8. pH dependence of k_{obsd} for the dissociation of $[CuLH_{-2}]$ with L = **2**.

Kinetics. As the two ligands behave differently in their equilibria, so they also do in their kinetics. Whereas **1** is so reactive that for Cu^{2+} the kinetics were too fast to be followed by stopped-flow techniques and only the reaction with Ni^{2+} could be measured, ligand **2** reacts so slowly that only the complexation and dissociation with Cu^{2+} are accessible to measurements.

Cu^{2+}–2 System. The kinetics of formation were measured in the pH region 5–5.8, in which the ligand exists in the monoprotonated form LH^+ (see Table I). As shown in Figure 7, the observed rate constant k_{obsd} is inversely proportional to $[H^+]$, indicating that L is the reactive species. Thus we can write eq 3, in which $k_L^{Cu} = 1.5\ M^{-1}\ s^{-1}$. This value is extremely low when

$$v_f = k_{obsd}[Cu^{2+}][LH^+]/[H^+] = k_{obsd}K_1[Cu^{2+}][L] = k_L^{Cu}[Cu^{2+}][L] \quad (3)$$

compared to the rate of the tetraamine analogue[19] in which the monoprotonated form already reacts faster than the fully deprotonated form of **2**. The reason for the slow incorporation of Cu^{2+} is due to the more rigid structure of **2** since the pyridine ring and the adjacent deprotonated amide groups form a planar arrangement.

The dissociation of the Cu^{2+} complex of **2** is slow and follows the pH dependence, as shown in Figure 8. The pH profile can be explained by assuming the reaction sequence in eq 4, from

$$[CuLH_{-2}] + H^+ \underset{\text{fast}}{\overset{K'}{\rightleftharpoons}} [CuLH_{-1}]^+ \xrightarrow[\text{slow}]{k_d} \text{products} \quad (4)$$

which the rate law in eq 5 can be derived, K' being the equilibrium

$$k_{obsd} = k_d[H^+]/(K' + [H^+]) \quad (5)$$

constant for the protonation of $[CuLH_{-2}]$ and k_d the dissociation rate constant of $[CuLH_{-1}]^+$. Nonlinear curve fitting of the experimental points gives $k_d = (3.3 \pm 0.2) \times 10^{-2}\ s^{-1}$ and $K' = 5.9 \pm 0.5$ M. We assume that the protonation takes place at one of the carbonyl oxygen atoms of the coordinated amide group, as has been proposed for analogous reactions,[24] and that this weakens the metal–ligand bond so that dissociation can then take place.

Ni^{2+}–1 System. The kinetics of the system **1** and Ni^{2+} have been followed from pH 5.5 to 8.5 (dissociation) and from pH 8.5 to 10.5 (formation). As usual for measurements done in the equilibrium region, k_{obsd} is the sum of the forward and reverse reactions.[25] The results shown in Figure 9 indicate that this is indeed true here. k_{obsd} has been fitted with a sequence of terms, which include formation and dissociation steps at the same time (eq 6). The best fitting gives $k_1 = (9.3 \pm 0.4) \times 10^7\ M^{-1}\ s^{-1}$,

$$k_{obsd} = k_1[H^+]^2/(k_2 + [H^+]) + k_3 + k_4/[H^+] \quad (6)$$

$k_2 = (3.9 \pm 0.5) \times 10^{-8}$ M, $k_3 = (6.9 \pm 0.6) \times 10^{-2}\ s^{-1}$, and k_4

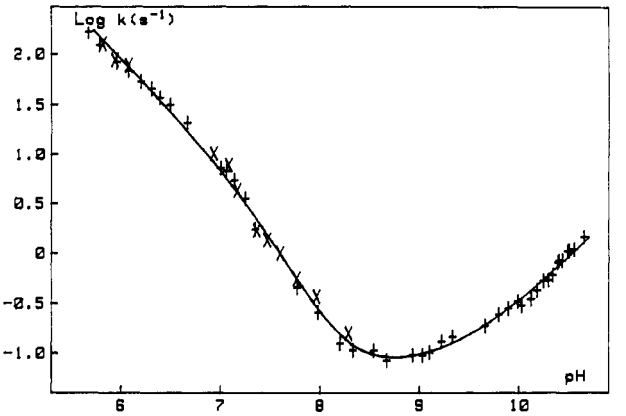

Figure 9. pH profile of k_{obsd} for the formation and dissociation of $[NiLH_{-2}]$ with L = **1**. The theoretical curve is calculated with the best constants given in the text.

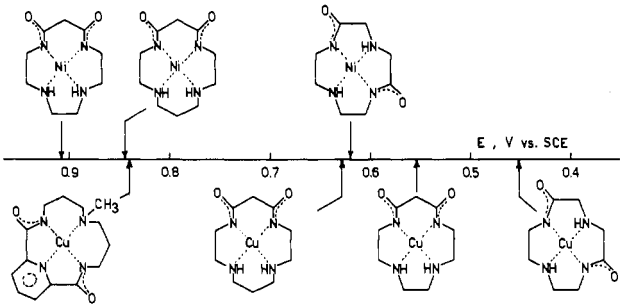

Figure 10. M(III)/M(II) redox couple potentials for the Ni and Cu complexes with different dioxo macrocycles (3.0 M $NaClO_4$, 25 °C).

$= (2.7 \pm 0.1) \times 10^{-11}\ M\ s^{-1}$. The dissociation of $[NiLH_{-2}]$ can be described with the sequence of protonation reactions shown in eq 7, which by applying the "steady state" approximation gives

$$[NiLH_{-2}] \underset{k_{-a}}{\overset{k_{+a}}{\rightleftharpoons}} [NiLH_{-1}]^+ \xrightarrow{k_b} \text{products} \quad (7)$$

eq 8. Thus by comparison of eq 8 with eq 6, $k_1 = k_{+a}$ and k_2

$$k_{obsd} = k_{+a}[H^+]^2/(k_{-a}/k_b + [H^+]) \quad (8)$$

$= k_{-a}/k_b$, both describing the dissociation reaction. The formation must start from NiL^{2+}, which rapidly forms when solutions of Ni^{2+} and **1** are mixed at pH <8.50; thus we can write eq 9, and the

$$[NiL]^{2+} + OH^- \xrightarrow{k_c} [NiLH_{-1}]^+ \xrightarrow{\text{fast}} [NiLH_{-2}] \quad (9)$$

rate constant becomes that shown in eq 10, with k_4 being the

$$k_{obsd} = k_c[OH^-] = k_cK_w/[H^+] = k_4/[H^+] \quad (10)$$

deprotonation rate constant of $[NiL]^{2+}$. Whether k_3 (eq 6), the pH-independent term found in the equilibrium region, is connected with the formation or dissociation is impossible to say. It is worthwhile to note that the protonation and deprotonation behavior of the Ni^{2+} complexes of **1** closely resembles those of open-chain amide complexes, as it has been observed for oligopeptides[26] and for other ligands containing amide groups.[27]

Formation of Trivalent Nickel and Copper Complexes. Coordination of Ni(II) and Cu(II) by deprotonated amido groups favors the access to the otherwise-elusive trivalent state. This was first discovered by Margerum et al. in the case of metal complexes with polypeptides.[28] Fairly stable Ni(III) and Cu(III) complexes with

(24) Buckingham, D. A.; Forster, D. M.; Sargeson, A. M. *J. Am. Chem. Soc.* **1969**, *91*, 3451–3456.
(25) Benson, S. W. "The Foundation of Chemical Kinetics"; McGraw-Hill, New York, 1960; p 96.
(26) Margerum, D. W.; Dukes, G. R. *Met. Ions Biol. Syst.* **1974**, *1*, 157.
(27) Zuberbühler, A. D.; Kaden, Th. A. *Helv. Chim. Acta* **1972**, *55*, 623–629.
(28) Margerum, D. W.; Chelappa, K. L.; Bossu, F. P.; Bruce, G. L. *J. Am. Chem. Soc.* **1975**, *97*, 6894–6896.

the dioxo tetraaza macrocycles **3**,[17] **4**,[12] and **1**[6] have been previously characterized through electrochemical studies.

In general, the Cu(II)/Cu(III) redox process displays a reversible or quasi-reversible behavior independent of the type and concentration of the supporting electrolyte; on the contrary, the corresponding Ni(II)/Ni(III) redox change, as judged from the shape of the CV profiles, shows a quasi-reversible pattern only at relatively high concentrations of supporting electrolyte. In Figure 10 are shown the values of the M(III)/M(II) redox couple potential measured by CV experiments in 3 M $NaClO_4$. The poorly coordinating perchlorate ion was employed to avoid complications due to the axial anion coordination in Ni(III) complexes and to make a proper comparison of the stabilizing effects of the two macrocycles on the trivalent nickel and copper cations.

The diagram in Figure 10 shows that the formation of trivalent copper complexes is favored with respect to that of the analogous nickel ones, inverting the trend normally observed (for instance in the case of fully saturated macrocycles).[12] This can be ascribed to the especially large CFSE contribution from which the Cu(II)/Cu(III) change profits in a tetragonal coordinative arrangement.[12]

Ligand ring size has a profound effect on the relative stability of trivalent nickel and copper complexes: for both metal ions the easiest access to the trivalent state occurs with the smallest 12-membered ligand (**1**).

The trend found in the case of copper (progressive stabilization of the trivalent species as the ring size decreases along the series 14-, 13-, 12-membered macrocycles) agrees with the drastic reduction of the size of the metal ion that occurs in the Cu(II) to Cu(III) (d^8, low spin) redox change. In particular, in the case of the 12-membered ring **1**, the metal ion, which in the divalent state is too large to fit the tetraaza cavity and lies over the N_4 plane, on oxidation becomes small enough to allow coplanar coordination by the macrocycle. This may explain the very low value of the Cu(III)/Cu(II) redox couple potential (the lowest found for copper polyaza macrocyclic complexes).

The interpretation of the trend for the corresponding nickel complexes is not straightforward. In this case, in fact, the oxidation of planar low-spin d^8 Ni(II) to octahedral low-spin d^7 Ni(III) does not involve contraction but a slight expansion of the ionic radius as estimated from Ni–N distances available for fully saturated tetraaza macrocyclic complexes.[29] In particular, the Ni(III) cation should fit better with the larger 14-membered dioxo macrocycle than the 13-membered one. Therefore, it may seem surprising that the greatest stabilization of the Ni(III) ion occurs with the smallest size macrocycle.

The Cu(III) complex of **2** is formed at a more positive potential than the complexes with the other dioxo tetraaza macrocycles. This can be ascribed to the reduced coordinating behavior of **2**, due to the presence of a pyridine rather than amine nitrogen atom in the donor set.

On controlled-potential electrolysis of a blue solution of the Cu^{II}–**1** system (adjusted at the minimum pH at which the [$CuLH_{-2}$] species is present at 100%, i.e. 8) performed by using platinum gauze as an anode to which a potential of +700 mV vs. SCE was imposed, the solution turns yellow-green, due to the formation of the Cu(III) complex. The Cu(III) spectrum (Figure 11) decays following a first-order reaction with a $t_{1/2}$ value of 132 min, restoring the spectrum, and the color, of the blue Cu(II) complex. The yellow-green Cu(III) solution can also be obtained by chemical oxidation, using $S_2O_8^{2-}$ as an oxidizing agent.

Analogous controlled-potential experiments performed on the Cu^{II}–**3** and Cu^{II}–**4** systems (solutions adjusted to the minimum pH that allows the formation of 100% of the [$CuLH_{-2}$] species) led to the formation of brown solutions of the trivalent complexes. The stability toward decomposition of the above species, estimated from the decay of the UV–visible spectrum, is smaller than that observed with the Cu(III) complex of **1**, $t_{1/2}$ values for both ligands (**3** and **4**) being about 20 min. The results indicate that the thermodynamically most stable complex, the [$CuLH_{-2}$] species of the Cu^{III}–**1** system, as judged from the less positive value of the Cu(III)/Cu(II) redox couple potential, is also the most stable from a kinetic point of view.

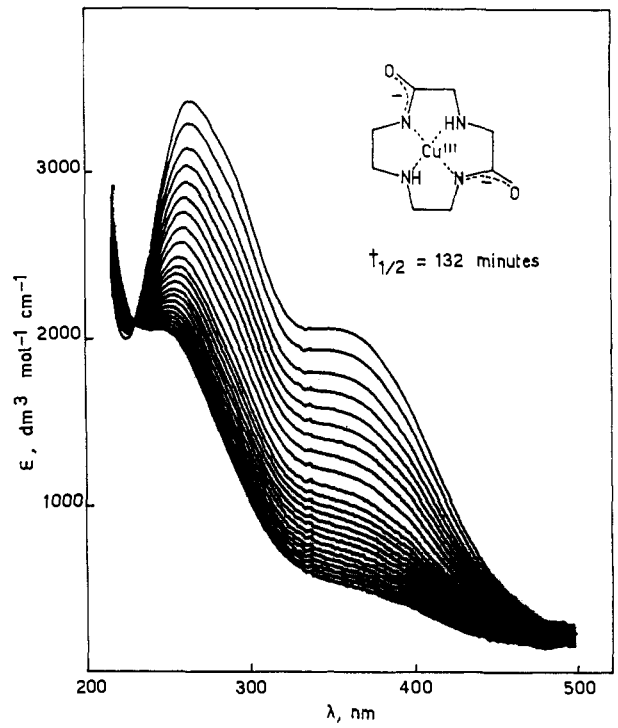

Figure 11. Decay of the Cu^{3+} complex with **1** in aqueous solution at 25 °C. Spectra were taken every 20 min.

Controlled-potential electrolysis experiments, performed by using a platinum anode, on Ni(II) dioxo macrocyclic solutions do not work well: in order to produce the brown solution of the Ni(III) complex, a potential much higher than the $E_{1/2}$(Ni(III)/Ni(II)) value (measured by CV using a carbon-paste electrode) must be imposed onto the anode. However, the integrated current signal does not reach a limiting value but increases constantly, indicating a parallel decomposition process. This behavior is probably due to the poor reversibility of the Ni(III)/Ni(II) redox change on the platinum surface.

Oxidation of Ni(II) dioxo tetraaza macrocyclic complexes to give the brown Ni(III) species can be performed through chemical oxidation using $Na_2S_2O_8$. In this case, the family of spectra of the Ni(III) solution, recorded as a function of time, did not show an isosbestic point, indicating ligand decomposition and metal extrusion and not a decay to the divalent complex. Similar behavior (no isosbestic point) was also observed for the Cu(III) solutions, when prepared through peroxydisulfate oxidation. In the case of nickel, the lasting time of the chemically generated Ni(III) complexes was also found to be seriously affected by the nature of the supporting electrolyte. In the most favorable situation (3 M KCl), half-lives of 30–40 min were measured.

Conclusions

A comparison of the ligating properties of **1** and **2** clearly shows that the more flexible ligand **1** gives a series of complexes with variable stoichiometry $[MLH]^{3+}$, $[ML]^{2+}$, $[MLH_{-1}]^{+}$, and $[MLH_{-2}]$ for Cu^{2+} and $[MLH]^{3+}$, $[ML]^{2+}$, and $[MLH_{-2}]$ for Ni^{2+}, whereas the more rigid ligand **2** forms only a Cu^{2+} complex of the type $[MLH_{-2}]$. The same trend is observed when one compares **1** with the two ligands **3** and **4**, which have cis arrangements of the amide groups. With these last two macrocycles only $[ML]^{2+}$ and $[MLH_{-2}]$ species were observed for Cu^{2+}, indicating that ligands **3** and **4** are somewhat more rigid than **1**.

The two ligands **1** and **2** also differ in their kinetics of complexation. The reactivity of ligand **2** is similar to that of the dioxo-free macrocycles, whereas **1** exhibits kinetics in which the

(29) Zeigerson, E.; Bar, I.; Bernstein, J.; Kirschenbaum, L. J.; Meyerstein, D. *Inorg. Chem.* **1982**, *21*, 73–80.

protonation and deprotonation of the amide groups are rate-determining steps, similar to what has previously been observed for open-chain ligands. Thus **2** has a predominant macrocyclic character, whereas **1** is controlled by the reactivity of the amide groups.

On the other hand, the attainment of the trivalent state for both nickel and copper complexes, which is greatly favored by the presence of deprotonated amido groups, is mainly dependent on the ring size but practically independent of the more or less rigid structure of the macrocycle.

Contribution from the Department of Chemistry,
Texas A&M University, College Station, Texas 77843

Gallium(III), Aluminum(III), and Zinc(II) Pyridoxal 5′-Phosphate Catalyzed Transamination and Dephosphonylation of 2-Amino-3-phosphonopropionic Acid

Bruno Szpoganicz† and Arthur E. Martell*

Received June 11, 1985

Kinetic studies of reactions of the Schiff bases (SB) formed from pyridoxal 5′-phosphate (PLP) and 2-amino-3-phosphonopropionic acid (APP) and of the 1:1:1 Zn(II)–SB–PDA system (PDA = 2,6-pyridinedicarboxylic acid), the 1:2 Ga(III)–SB system, and the 1:2 Al(III)–SB system have been carried out. Formation and disappearance of a ketimine intermediate and its complexes were followed by proton NMR and ^{31}P NMR. The reaction occurs in two distinct sequential steps: transamination and dephosphonylation. The specific rate constants for individual species of the metal-free systems are $k_{H_4SB} = 1.64 \times 10^{-4}$ s^{-1}, $k_{H_3SB} = 7.56 \times 10^{-5}$ s^{-1}, and $k_{H_2SB} = 2.34 \times 10^{-5}$ s^{-1} for the transamination step. The values for k_{HSB} and k_{SB} are about zero. The corresponding dephosphonylation rate constants are $k'_{H_4SB} = 4.27 \times 10^{-6}$ s^{-1}, $k'_{H_3SB} = 1.26 \times 10^{-6}$ s^{-1}, and $k'_{H_2SB} = 6.84 \times 10^{-7}$ s^{-1}. The values for k'_{HSB} and k'_{SB} are about zero. Transamination and dephosphonylation reactions proceed more rapidly for Ga(III) complexes than for those of Al(III) and Zn(II). The specific transamination rate constants for the individual species of the 1:2 Ga(III)–SB system are $k_{Ga(H_3SB)_2} = 4.66 \times 10^{-4}$ s^{-1}, $k_{GaH_5(SB)_2} = 3.51 \times 10^{-4}$ s^{-1}, $k_{Ga(H_2SB)_2} = 3.13 \times 10^{-4}$ s^{-1}, $k_{GaH_3(SB)_2} = 3.13 \times 10^{-4}$ s^{-1}, $k_{Ga(HSB)_2} = 3.15 \times 10^{-4}$ s^{-1}, $k_{GaH(SB)_2} = 2.20 \times 10^{-4}$ s^{-1}, and $k_{Ga(SB)_2} = 3.12 \times 10^{-5}$ s^{-1}. The specific rate constants for the dephosphonylation step are $k_{GaH_5(SB)_2} = 5.2 \times 10^{-6}$ s^{-1}, $k_{Ga(H_2SB)_2} = 5.20 \times 10^{-6}$ s^{-1}, $k_{GaH_3(SB)_2} = 5.17 \times 10^{-6}$ s^{-1}, $k_{Ga(HSB)_2} = 5.09 \times 10^{-6}$ s^{-1}, $k_{GaH(SB)_2} = 2.53 \times 10^{-6}$ s^{-1}, and $k_{Ga(SB)_2} = 4.92 \times 10^{-7}$ s^{-1}. The results show that the most active species are those in which the carboxylate group of the amino acid moiety of the SB ligand is coordinated to the metal ion and the phosphonate is not coordinated.

Introduction

This paper describes kinetic studies of transamination and dephosphonylation of 2-amino-3-phosphonopropionic acid (APP) catalyzed by pyridoxal 5′-phosphate(PLP) and Zn(II), Al(III), or Ga(III) as the culmination of a series of comprehensive investigations of reactions of the PLP–APP system.[1-3] The extensive equilibrium studies conducted on PLP–APP, Zn(II)–PLP–APP–PDA (PDA = 2,6-pyridinecarboxylic acid), Al(III)–PLP–APP, and Ga(III)–PLP–APP, systems have provided a complete description of molecular species formed as a function of p[H] and of concentrations of the components. Preliminary spectrophotometric studies on APP demonstrated metal ion and pyridoxal catalysis of dephosphonylation, and a general reaction mechanism was proposed.[4,5] The reaction pathway suggested resembles the mechanism proposed for the pyridoxal-catalyzed β-decarboxylation of aspartic acid.[6,7] The purpose of this study is to measure the reaction kinetics, relate the reaction rate constants to the active species in solution, and, if possible, further clarify the reaction mechanism. Another objective of this investigation is to detect any intermediates formed during the reaction to provide additional information characterizing the nature of the reactions that occur with and without metal ions. The detection of intermediates by nuclear magnetic resonance in the metal ion–vitamin B_6 systems has been carried out for other reaction types.[7,8] Recently, the characterization of a general intermediate in the transamination reaction has been described.[9]

There are several advantages in using PLP rather than PL as a catalyst in the reactions being studied. The degree of formation of Schiff base intermediates is much higher with PLP. Also the phosphate ester moiety of vitamin B_6 increases solubility in water for the Schiff base as well as for its complexes. The metal complexes formed with the SB of PLP have less tendency to form neutral compounds, which could precipitate, than do those formed with the Schiff bases of pyridoxal.

Experimental Section

Materials. Pyridoxal 5′-phosphate was obtained from Sigma Chemical Company. 2-Amino-3-phosphonopropionic acid was purchased from Calbiochem-Behring Corp. Aluminum sulfate, hydrochloric acid, and potassium chloride were obtained from Fisher Scientific Co. Gallium metal was purchased from D. F. Goldsmith Chemical Metal Corp. Potassium deuteroxide (KOD) 40%, deuterium oxide (D_2O) 99.8% D, and deuterium chloride (DCl) were obtained from Aldrich Chemical Co., Inc. CO_2-free potassium hydroxide was obtained from J. T. Baker Chemical Co.

Potentiometric Equilibrium Determinations. A standard Al(III) solution, having a concentration of about 10^{-2} M, was prepared from reagent grade aluminum(III) sulfate octadecahydrate ($Al_2(SO_4)_3 \cdot 18H_2O$) and was standardized by titration with the disodium salt of EDTA.[10] Some HCl was added to avoid hydrolysis. Standard gallium(III) solutions were prepared by dissolving an accurately weighted quantity of 99.99% pure gallium metal in concentrated HCl. The exact amount of excess hydrochloric acid in the Al(III) and Ga(III) solutions was determined by a Gran's plot of $(V_0 + V_{KOH}) \times 10^{-pH}$ vs. V_{KOH}, where V_0 = the initial volume of the Al(III) or Ga(III) solution and V_{KOH} is the volume of added standard KOH. The intercept on the abscissa obtained by extrapolating the straight-line portion of the plot is a direct measure of the excess acid present.[11] The excess acid was also checked by the procedure of Harris and Martell.[12]

Samples of about 0.10 and 0.20 mmol of APP and PLP and 0.10 mmol of Al(III) or Ga(III) were diluted with 50 mL of double distilled water in a sealed, thermostated (25.0 ± 0.05 °C) potentiometric titration vessel equipped with a Sargent silver–silver chloride glass electrode and a calomel reference electrode, N_2 inlet and bubbler outlet, and a gradu-

† Abstracted in part from a dissertation submitted by Bruno Szpoganicz to the faculty of Texas A&M University in partial fullfillment of the requirements for the degree of Doctor of Philosophy.

(1) Szpoganicz, B.; Martell, A. E. *J. Am. Chem. Soc.* **1984**, *106*, 5513.
(2) Szpoganicz, B.; Martell, A. E. *Inorg. Chem.* **1984**, *23*, 4442.
(3) Szpoganicz, B.; Martell, A. E. *Inorg. Chem.* **1985**, *24*, 2414.
(4) Langohr, M. F.; Martell, A. E. *J. Chem. Soc., Chem. Commun.* **1977**, 343.
(5) Langohr, M. R.; Martell, A. E.; Tatsumoto, K. *Inorg. Chim. Acta* **1985**, *108*, 105.
(6) Sakkab, N. Y.; Martell, A. E. *Bioinorg. Chem.* **1975**, *5*, 67.
(7) Martell, A. E. *Adv. Enzymol. Relat. Areas Mol. Biol.* **1982**, *53*, 163.
(8) Abbott, E. D.; Martell, A. E. *J. Am. Chem. Soc.* **1973**, *95*, 5014.
(9) Taylor, P.; Martell, A. E. *Inorg. Chem.* **1984**, *23*, 2734.
(10) Schwarzenbach, G.; Flaschka, H. "Complexometric Titration"; Methuen Co. Ltd.: London, 1969.
(11) Rossotti, F. J. C.; Rossotti, H. *J. Chem. Educ.* **1965**, *42*, 375.
(12) Harris, W. R.; Martell, A. E. *Inorg. Chem.* **1976**, *15*, 713.

0020-1669/86/1325-0327$01.50/0